Rev. Mexicana Astron. Astrof., 9, 53-64 (1984)

THIRTEEN-COLOR PHOTOMETRY OF B-TYPE STARS

W.J. Schuster

Instituto de Astronomía
Universidad Nacional Autónoma de México

Received 1983 September 27

RESUMEN

Presentamos datos fundamentales para el estudio de estrellas tipo B. Se presentan cocientes de enrojecimiento interestelar, colores intrínsecos, estrellas de comparación, índices libres de enrojecimiento, y calibraciones para los tipos espectrales MK, temperaturas efectivas, y magnitudes absolutas visuales. En particular, discutimos brevemente el uso de fotometría 13C en la medición de distancias estelares y en el estudio de excesos intrínsecos de estrellas Be y de estrellas con cascarón (shell).

ABSTRACT

We present data fundamental for the study of B-type stars. Interstellar reddening ratios, intrinsic colors, comparison stars, reddening-free indices, and calibrations for MK spectral type, effective temperature, and absolute visual magnitude are given. In particular we discuss briefly the use of 13C photometry for measuring stellar distances and for studying intrinsic excesses of Be and shell stars.

Key words: **PHOTOMETRY – STARS B-TYPES**

I. INTRODUCTION

In 1979 we began a long-term program of monitoring the photometric variability of Be stars using the 13-color (13C) photometric system (Schuster and Alvarez 1983). We have found the system to be particularly useful for measuring the continuum variability of these stars, such as variations in the Balmer jump, in the visual magnitudes, and in the near infrared ($\sim$ 8000 A) (Schuster and Alvarez 1983; Alvarez and Schuster 1982). We have also discovered evidence that these stars are most variable at those wavelengths where their intrinsic excesses are largest. However, our method of determing intrinsic excesses for Be stars in the 13C system has to date been somewhat rudimentary due to the lack of mean intrinsic colors for normal B stars, such as exist for Johnson broad-band photometry (Fitzgerald 1970; Johnson 1966) and for Strömgren intermediate-band photometry (Crawford 1978).

More than 1500 stars have been observed with the 13C system (mainly Johnson and Mitchell 1975; also see Schuster 1982*b* for other references), but little has been done to calibrate this photometry. Schuster (1976, 1979*a*, 1979*b*) obtained mean colors and several calibrations for F- and G-type stars using members of the Hyades cluster, solar-type stars and subdwarf stars. Johnson and Mitchell (1975) give an absolute energy calibration. Also, seven of the 13C filters are similar to those used by Borgman (1960), and Borgman and Blaauw (1964) do give calibrations concerning absolute magnitudes and intrinsic colors for early-type stars. However, the seven filters are not identical in the two systems, the zero-points of the colors are totally different, and the 13C photometry has six additional red and near-infrared filters. So, although the 13C system of intermediate-band photometry was originally developed for the study and classification of early-type stars (Johnson, Mitchell and Latham 1967; Mitchell and Johnson 1969), little has been done to prepare a basis for such work.

In this paper we hope to fill part of this void. We give interstellar reddening ratios, intrinsic mean colors and several calibrations concerning MK spectral types, effective temperatures, and luminosities of B stars. With this basis we can attack the Be-star problem with more assurance, and several papers will follow. Also, other investigators who wish to study B stars, photometric classification, photometric distances, and galactic spiral structure using 13C photometry will find our results most useful.

II. OUR DATA BASE

To obtain results as precise and uniform as possible, we have taken our data from only a few sources, catalogues with first-source data or those with data selected for high quality or homogeneity. Our sources for 13C data are the defining observations of Johnson and Mitchell (1975; based on the earlier publications of Johnson, Mitchell and Latham 1967; Mitchell and Johnson 1969) plus a few observations of O-type and early B stars by Schuster (1982*a*) and A supergiants by Schuster (1983). All of the northern observations of Johnson and Mitchell, most of the southern, and all of the observations of Schuster were made with the same photometers, filters and detectors, and so are "...homogeneous to an unusual degree" (Johnson and Mitchell 1975). A few of the

southern observations included in Johnson and Mitchell (1975) were made by Mendoza (1971) using filters made at the same time as those which define the 13C system and using different detectors. Overlapping observations between those of Mendoza and those made with the original photometers show no systematic differences (Mendoza 1971; Johnson and Mitchell 1975).

We have used *UBV* photometry extensively in these analyses to calculate color excesses (E($B-V$) and E($U-B$)), to make corrections for interstellar reddening, to derive intrinsic colors for supergiants and to check our intrinsic 13C colors for dwarfs, subgiants and giants. We have taken nearly all of our *UBV* photometry from only two sources, Johnson *et al.* (1966), which is one of the primary defining data sets for *UBV* photometry, and Nicolet (1978) who gives homogeneous *UBV* data. Only a very few *B-V* values for supergiants were taken from Hoffleit and Jaschek (1982).

For broad-band intrinsic colors we have used Fitzgerald (1970) and Johnson (1966). Fitzgerald worked with a larger data set both in *UBV* observations and MK spectral-luminosity classes, and so his intrinsic *UBV* colors have been preferred over those of Johnson. For early *B*-type main sequence stars the intrinsic $B-V$ values of Fitzgerald and Johnson do not differ; for late *B*-type dwarfs there are differences of only 0.01 or 0.02 mag. For $U-B$ intrinsic colors of main sequence stars deviations between the two data sets reach + 0.05 and −0.06 mag but are not systematic. For supergiants, differences as large as 0.03 mag for intrinsic $B-V$ and as large as 0.10 for $U-B$ were derived. For intrinsic *VRI* colors we have used exclusively the values of Johnson (1966) in our comparisons.

In our reddening study and spectral-color relationships, we have used the selected spectral types of Jaschek (1981) as our primary source, but have made many comparisons with those of Johnson and Mitchell (1975) and of Hoffleit and Jaschek (1982). None of these references include first source data but rather spectral types selected from other sources; generally those measured by W.W. Morgan are given high weight. Agreement among the spectral-luminosity types of these three references is very good. Nearly 400 stars were compared between Jaschek (1981) and Johnson and Mitchell (1975), and only eleven showed differences in luminosity as large as two classes (from V to III, for example). Hereafter the term "spectral type" will be designated by "Sp", and will refer to a complete spectral-luminosity class.

III. INTERSTELLAR REDDENING RATIOS

In Schuster (1982*b*) we gave preliminary reddening ratios for 13C photometry by comparing the effective wavelengths of the filters to reddening curves of several previous investigations (Whitford 1958; Whiteoak 1966; Johnson 1977; Borgman 1961). Here we derive our final reddening ratios using the method of reddening pairs. We have searched for pairs, or groups, of stars with equivalent MK classifications (equal spectral and luminosity types) but with large differences in interstellar reddening. Twelve groups of early-type stars (B0-F0) were found with ranges in E($B-V$) of at least + 0.25 mag. Two to eight stars belong to each group with 39 stars in total. Eight groups contain supergiants, and there is one group each for main sequence stars, subgiants, giants and bright giants. Linear regressions on the data were made, and the average reddening ratios are given in Table 1 with a comparison to the preliminary values. We have tied the reddening ratios to those of the Johnson broad-band system by including $B-V$ in our analyses.

Variations in the interstellar reddening law from region to region in the sky have been reported (Johnson 1977). Within each of our reddening groups the stars do not necessarily come from the same region of sky, and the most reddened stars of the different groups come from several different regions. If the reported variations are real, the values of Table 1 represent only an average interstellar reddening law which will be most useful for statistical studies of our Galaxy. However, the variation among the values going into the averages of Table 1 is small, ±0.02 to ±0.05 mag standard deviation for a single determination, so that the results of Table 1 can in any case be used to obtain results for individual stars as long as they are not too reddened (E(*33–63*) $\lesssim$ 1.0) and not from regions with a peculiar reddening law, such as the Orion Sword region.

IV. INTRINSIC MEAN COLORS

Intrinsic 13-color photometry has been derived for stars in the spectral range O9-A7 following the precepts of Fitzgerald (1970) with a few modifications to account for our larger number of filters and smaller number of observations. Our first step was to select our data set so as to work with B stars as normal as possible, having

TABLE 1

FINAL MEAN INTERSTELLAR REDDENING RATIOS[a]

Color	Reddening Ratio	Preliminary Value[b]
33–63	1.901	1.9
33–52	1.317	1.3
35–52	1.171	1.15
37–52	0.960	1.0
40–52	0.817	0.8
45–52	0.416	0.4
52–58	0.346	0.35
52–63	0.584	0.6
52–72	0.842	0.9
52–80	1.068	1.1
52–86	1.203	1.25
52–99	1.433	1.55
52–110	1.542	1.7
B–V	0.749	0.75
45–63	1.000	1.00

a. Normalized for *45–63* .
b. Schuster (1982).

egular MK spectral-luminosity classes and good photometry. Be stars, shell stars, stars with peculiar or uncertain pectral types, and stars with contaminated or questionible photometry were eliminated. However, all supergiants were used without any selection since the set was particularly small. Of approximately 650 stars available o us in the spectral range O9-A7, approximately 28% were removed prior to the derivation of the two-color elationships; another 3%, stars with composite spectra, were removed prior to the spectral-color relationships. Our final data set contained 210 dwarf stars, 120 subgiants, 61 giants and 57 supergiants; for the two-color iagrams involving the six red and infrared filters (6RC) hese numbers were reduced further by 56, 36, 7, and 2, respectively. Many of the stars observed in the southern emisphere by Mendoza with the blue photometer (8C) ave not been observed with the 6RC photometer. The bove numbers are fairly small but include all of the righter, closer, and least-reddened stars down to fifth isual magnitude in the northern sky and fourth visual nagnitude in the south (Johnson and Mitchell 1975).

Derivation of the intrinsic mean colors was carried ut in two steps. First, the two-color relations were obained using (*33–63*) to interpolate the intrinsic mean alues for the usual 13C colors. Second, the intrinsic pectral-color relations, $(33-63)_0$ versus MK spectral ype, were derived. We selected (*33–63*) as our interolating color since it has a large range for B-type stars nd is strictly an 8C color. We divided the process into wo parts for greater precision. Using the method of the lue-most envelope, a two-color diagram gives much reater precision for the intrinsic colors than a spectralolor diagram, since photometric observing errors have nuch less effect than MK classification errors (see Figure 2 in Fitzgerald 1970, and the accompanying discussion).

Four methods were used to derive the intrinsic colors ccording to ideas given in Fitzgerald (1970). The intrinic two-color relations were obtained and checked using he following three criteria: (a) stars within 100 parsecs, b) the blue-most envelope (plus a 2σ correction), and c) 13C colors corrected for interstellar reddening using $E(B-V)$. The intrinsic spectral-color relations resulted rom these three methods plus: (d) groups of stars with onstant spectral-luminosity types projected along the eddening trajectories to the intrinsic relations in our wo-color diagrams.

Eggen (1963) and Fitzgerald (1968, 1970) have shown that there is negligible interstellar reddening for all directions out to 50 pc, and also out to 100 pc except in a few special directions where there is slight reddening. For Sp of approximately B8 (V, IV and III) and later, this method has carried considerable weight in deriving the 13C intrinsic colors. For the earlier B stars few are found within 100 pc.

The blue-most envelope method worked best for the main sequence and subgiant stars where sufficient numbers were available to apply statistical corrections. In the two-color and spectral-color diagrams we drew the blue-most envelopes excluding only approximately 5% of the stars, and then corrected this envelope redward by 2σ, where σ is the estimated observational error. For the photometric data the σ's were taken from Schuster (1982*b*) and for the Sp σ was taken as 0.6 to 1.0 spectral division according to the results of Jaschek and Jaschek (1973). The 2σ correction gives precise intrinsic colors when a significant fraction of the stars are unreddened, but overcorrects otherwise. For the late B stars the full 2σ correction was applied, but for the early B stars the blue-most envelope was taken without correction to give the intrinsic colors, and for the middle B stars the correction was interpolated. For dwarf, subgiant and giant stars with Sp later than B8 the intrinsic colors from this method were in excellent agreement with those given by the stars within 100 pc.

The method of using $E(B-V)$, or $E(U-B)$, to correct our 13C photometry for reddening is not an independent method since the results will depend on the intrinsic *UBV* colors of Fitzgerald (1970). For dwarf and subgiant stars this method has been used as a check for systematic errors, and in a few cases has lead to corrections of 0.01 or 0.02 mag in our intrinsic two-color relations for early B-type stars. For giant stars, whose total number is smaller, and in the spectral-color diagrams, this method has carried more weight.

For supergiants our sample is small, none are found within 100 pc, the blue-most envelopes are not well defined, and nearly all are somewhat reddened. So, for these stars the intrinsic two-color and spectral-color relations were found using strictly method (c) above. Hence, for supergiants our results do not represent an independent determination of intrinsic color, but depend directly upon the *UBV* intrinsic colors of Fitzgerald (1970).

For the final mean intrinsic two-color relations we have smoothed slightly the results given by the above three methods, and the final results are given in Tables 2 through 6. Insufficient data were available to define intrinsic colors for bright giants (luminosity class II) and for intermediate luminosity classes, such as IV-V, III-IV, II-III, and Iab. A few stars with classifications of IV-V were grouped with the subgiant stars, but they represent less than 15% of the total number. Also, a very few stars with classifications III-IV and II-III were grouped with the giant stars (less than 10%of the total).

In the spectral-color diagrams the scatter from the above three methods was larger, due to errors in the MK spectral types, than for the two-color diagrams, and an unbiased smoothing of the data was more difficult. However, once the intrinsic two-color relations had been obtained, method (d) could be used to better define the Sp-$(33-63)_0$ relation. Six 13C two-color diagrams were used, namely (*40–52*), (*45–52*), (*52–58*), (*52–72*), (*52–80*) and (*52–86*) versus (*33–63*); these are the diagrams for which the intrinsic colors are best defined

TABLE 2

MEAN UNREDDENED 13-COLOR PHOTOMETRY, MAIN SEQUENCE (V)

Sp	*33–63*	*33–52*	*35–52*	*37–52*	*40–52*	*45–52*	*52–58*	*52–63*	*52–72*	*52–80*	*52–86*	*52–99*	*52–110*
O9	-2.04	-1.87	-1.74	-1.13	-0.39	-0.09	-0.10	-0.18	-0.25	-0.33	-0.40	-0.61	-0.63
B0	-1.88	-1.71	-1.59	-1.04	-0.36	-0.09	-0.10	-0.17	-0.24	-0.31	-0.37	-0.56	-0.58
B0.5	-1.80	-1.63	-1.51	-1.00	-0.35	-0.08	-0.10	-0.16	-0.24	-0.30	-0.36	-0.53	-0.56
B1	-1.73	-1.57	-1.45	-0.95	-0.33	-0.08	-0.09	-0.16	-0.23	-0.30	-0.34	-0.51	-0.54
B1.5	-1.65	-1.49	-1.37	-0.91	-0.32	-0.08	-0.09	-0.15	-0.23	-0.29	-0.33	-0.49	-0.51
B2	-1.57	-1.41	-1.30	-0.86	-0.31	-0.08	-0.09	-0.15	-0.22	-0.27	-0.31	-0.46	-0.49
B2.5	-1.49	-1.33	-1.22	-0.82	-0.29	-0.08	-0.09	-0.14	-0.21	-0.26	-0.29	-0.44	-0.47
B3	-1.42	-1.27	-1.16	-0.78	-0.28	-0.07	-0.08	-0.13	-0.21	-0.25	-0.28	-0.42	-0.45
B4	-1.26	-1.12	-1.03	-0.69	-0.25	-0.07	-0.08	-0.12	-0.19	-0.23	-0.25	-0.37	-0.40
B5	-1.11	-0.99	-0.90	-0.61	-0.22	-0.06	-0.07	-0.10	-0.17	-0.20	-0.22	-0.32	-0.36
B6	-0.96	-0.86	-0.79	-0.54	-0.20	-0.05	-0.06	-0.09	-0.15	-0.18	-0.19	-0.28	-0.32
B7	-0.79	-0.72	-0.65	-0.46	-0.17	-0.04	-0.05	-0.07	-0.13	-0.14	-0.16	-0.23	-0.27
B8	-0.57	-0.53	-0.48	-0.35	-0.13	-0.03	-0.04	-0.05	-0.09	-0.10	-0.11	-0.16	-0.20
B9	-0.30	-0.28	-0.25	-0.20	-0.08	-0.01	-0.02	-0.02	-0.04	-0.04	-0.06	-0.08	-0.11
B9.5	-0.12	-0.12	-0.11	-0.09	-0.04	0.00	0.00	-0.01	-0.01	0.00	-0.02	-0.02	-0.03
A0	-0.02	-0.03	-0.03	-0.03	-0.01	+0.01	+0.01	+0.01	+0.01	+0.02	+0.01	+0.01	+0.02
A1	+0.08	+0.05	+0.05	+0.03	+0.02	+0.01	+0.02	+0.03	+0.03	+0.04	+0.04	+0.06	+0.07
A2	+0.15	+0.10	+0.09	+0.08	+0.05	+0.02	+0.03	+0.04	+0.05	+0.07	+0.08	+0.09	+0.11
A3	+0.24	+0.16	+0.14	+0.12	+0.09	+0.04	+0.05	+0.07	+0.09	+0.11	+0.13	+0.14	+0.16
A4	+0.32	+0.20	+0.17	+0.16	+0.15	+0.05	+0.07	+0.11	+0.13	+0.16	+0.18	+0.19	+0.22
A5	+0.37	+0.24	+0.19	+0.19	+0.19	+0.07	+0.08	+0.13	+0.17	+0.21	+0.23	+0.24	+0.28
A6	+0.41	+0.26	+0.21	+0.21	+0.22	+0.08	+0.10	+0.15	+0.21	+0.26	+0.26	+0.30	+0.34
A7	+0.45	+0.29	+0.23	+0.24	+0.25	+0.09	+0.11	+0.17	+0.25	+0.31	+0.31	+0.38	+0.41

TABLE 3

MEAN UNREDDENED 13-COLOR PHOTOMETRY, SUBGIANTS (IV, IV-V)

Sp	*33–63*	*33–52*	*35–52*	*37–52*	*40–52*	*45–52*	*52–58*	*52–63*	*52–72*	*52–80*	*52–86*	*52–99*	*52-110*
O9	-2.03	-1.83	-1.69	-1.14	-0.38	-0.10	-0.11	-0.18	-0.24	-0.35	-0.41	-0.59	-0.61
B0	-1.88	-1.70	-1.56	-1.05	-0.36	-0.10	-0.10	-0.17	-0.23	-0.32	-0.38	-0.55	-0.57
B0.5	-1.80	-1.62	-1.49	-1.00	-0.35	-0.10	-0.10	-0.16	-0.23	-0.31	-0.37	-0.53	-0.55
B1	-1.73	-1.56	-1.43	-0.96	-0.34	-0.10	-0.10	-0.16	-0.22	-0.30	-0.36	-0.52	-0.53
B1.5	-1.65	-1.49	-1.36	-0.91	-0.33	-0.09	-0.10	-0.15	-0.21	-0.28	-0.34	-0.50	-0.51
B2	-1.57	-1.42	-1.29	-0.87	-0.32	-0.09	-0.09	-0.14	-0.20	-0.27	-0.33	-0.47	-0.48
B2.5	-1.50	-1.35	-1.23	-0.83	-0.32	-0.09	-0.09	-0.13	-0.20	-0.26	-0.31	-0.45	-0.46
B3	-1.42	-1.28	-1.16	-0.79	-0.31	-0.09	-0.08	-0.13	-0.19	-0.24	-0.30	-0.43	-0.44
B4	-1.27	-1.15	-1.04	-0.71	-0.28	-0.08	-0.07	-0.11	-0.17	-0.22	-0.26	-0.38	-0.39
B5	-1.12	-1.02	-0.92	-0.63	-0.25	-0.07	-0.06	-0.10	-0.15	-0.19	-0.23	-0.33	-0.34
B6	-0.97	-0.88	-0.79	-0.55	-0.21	-0.06	-0.05	-0.09	-0.12	-0.17	-0.20	-0.28	-0.29
B7	-0.82	-0.75	-0.67	-0.47	-0.19	-0.05	-0.04	-0.07	-0.10	-0.14	-0.17	-0.24	-0.24
B8	-0.64	-0.59	-0.52	-0.38	-0.15	-0.04	-0.03	-0.05	-0.08	-0.11	-0.13	-0.18	-0.18
B9	-0.41	-0.38	-0.33	-0.26	-0.10	-0.03	-0.02	-0.03	-0.05	-0.07	-0.08	-0.10	-0.11
B9.5	-0.18	-0.17	-0.15	-0.15	-0.06	-0.01	0.00	-0.01	-0.02	-0.03	-0.03	-0.04	-0.04
A0	-0.04	-0.05	-0.04	-0.08	-0.03	0.00	+0.01	0.00	0.00	0.00	0.00	0.00	+0.01
A1	+0.11	+0.08	+0.07	0.00	+0.01	+0.01	+0.02	+0.02	+0.03	+0.05	+0.05	+0.07	+0.08
A2	+0.21	+0.15	+0.12	+0.06	+0.05	+0.02	+0.04	+0.05	+0.07	+0.10	+0.10	+0.12	+0.13
A3	+0.28	+0.20	+0.15	+0.10	+0.09	+0.04	+0.05	+0.08	+0.11	+0.14	+0.14	+0.17	+0.19
A4	+0.33	+0.23	+0.18	+0.14	+0.13	+0.05	+0.07	+0.11	+0.14	+0.18	+0.18	+0.21	+0.25
A5	+0.38	+0.25	+0.20	+0.17	+0.17	+0.06	+0.09	+0.13	+0.17	+0.22	+0.23	+0.26	+0.30
A6	+0.42	+0.27	+0.22	+0.19	+0.20	+0.08	+0.10	+0.15	+0.20	+0.26	+0.27	+0.30	+0.34
A7	+0.47	+0.29	+0.24	+0.22	+0.23	+0.10	+0.12	+0.18	+0.24	+0.31	+0.32	+0.36	+0.40

TABLE 4

MEAN UNREDDENED 13-COLOR PHOTOMETRY, GIANTS (III, II-III, III-IV)

Sp	*33–63*	*33–52*	*35–52*	*37–52*	*40–52*	*45–52*	*52–58*	*52–63*	*52–72*	*52–80*	*52–86*	*52–99*	*52-110*
O9	-2.11	-1.92	-1.77	-1.16	-0.40	-0.11	-0.11	-0.17	-0.26	-0.34	-0.41	-0.61	-0.63
B0	-1.94	-1.77	-1.63	-1.07	-0.37	-0.10	-0.10	-0.16	-0.24	-0.31	-0.38	-0.56	-0.58
B0.5	-1.86	-1.69	-1.56	-1.03	-0.36	-0.10	-0.10	-0.15	-0.23	-0.30	-0.37	-0.54	-0.55
B1	-1.77	-1.62	-1.49	-0.99	-0.35	-0.10	-0.09	-0.15	-0.22	-0.28	-0.35	-0.51	-0.53
B1.5	-1.68	-1.53	-1.42	-0.95	-0.33	-0.09	-0.09	-0.14	-0.21	-0.27	-0.33	-0.49	-0.50
B2	-1.60	-1.46	-1.35	-0.91	-0.32	-0.09	-0.09	-0.13	-0.20	-0.26	-0.32	-0.46	-0.48
B2.5	-1.51	-1.38	-1.28	-0.86	-0.30	-0.08	-0.08	-0.13	-0.19	-0.24	-0.30	-0.44	-0.45
B3	-1.42	-1.30	-1.20	-0.82	-0.29	-0.08	-0.08	-0.12	-0.18	-0.23	-0.28	-0.41	-0.43
B4	-1.25	-1.15	-1.06	-0.73	-0.26	-0.07	-0.07	-0.10	-0.16	-0.20	-0.25	-0.36	-0.38
B5	-1.08	-1.00	-0.92	-0.65	-0.23	-0.06	-0.06	-0.09	-0.14	-0.18	-0.21	-0.31	-0.33
B6	-0.92	-0.86	-0.79	-0.57	-0.21	-0.05	-0.05	-0.08	-0.12	-0.15	-0.18	-0.26	-0.28
B7	-0.75	-0.70	-0.65	-0.49	-0.18	-0.04	-0.04	-0.07	-0.10	-0.13	-0.15	-0.21	-0.23
B8	-0.58	-0.54	-0.51	-0.41	-0.15	-0.04	-0.03	-0.05	-0.08	-0.10	-0.12	-0.16	-0.19
B9	-0.36	-0.33	-0.32	-0.29	-0.11	-0.02	-0.02	-0.04	-0.06	-0.07	-0.08	-0.10	-0.12
B9.5	-0.23	-0.20	-0.20	-0.21	-0.09	-0.01	-0.01	-0.03	-0.04	-0.05	-0.05	-0.06	-0.08
A0	-0.08	-0.06	-0.07	-0.13	-0.06	0.00	0.00	-0.01	-0.03	-0.03	-0.02	-0.02	-0.04
A1	+0.14	+0.11	+0.09	0.00	0.00	+0.01	+0.02	+0.03	+0.01	+0.01	+0.03	+0.05	+0.04
A2	+0.25	+0.19	+0.16	+0.07	+0.05	+0.03	+0.03	+0.06	+0.04	+0.05	+0.07	+0.10	+0.10
A3	+0.34	+0.25	+0.20	+0.12	+0.09	+0.04	+0.05	+0.09	+0.09	+0.12	+0.13	+0.16	+0.17
A4	+0.39	+0.29	+0.23	+0.15	+0.12	+0.05	+0.06	+0.11	+0.12	+0.16	+0.18	+0.21	+0.23
A5	+0.42	+0.31	+0.25	+0.17	+0.15	+0.06	+0.07	+0.12	+0.15	+0.19	+0.21	+0.24	+0.27
A6	+0.43	+0.32	+0.25	+0.17	+0.16	+0.06	+0.07	+0.12	+0.16	+0.21	+0.22	+0.26	+0.29
A7	+0.44	+0.32	+0.26	+0.18	+0.17	+0.06	+0.08	+0.13	+0.16	+0.22	+0.24	+0.27	+0.30

TABLE 5

MEAN UNREDDENED 13-COLOR PHOTOMETRY, SUPERGIANTS (Ib)

Sp	*33–63*	*33–52*	*35–52*	*37–52*	*40–52*	*45–52*	*52–58*	*52–63*	*52–72*	*52–80*	*52–86*	*52–99*	*52–110*
O9	-1.98	-1.84	-1.71	-1.10	-0.40	-0.11	-0.09	-0.14	-0.21	-0.28	-0.37	-0.52	-0.51
B0	-1.80	-1.69	-1.57	-1.02	-0.33	-0.07	-0.06	-0.10	-0.16	-0.22	-0.29	-0.43	-0.45
B0.5	-1.72	-1.63	-1.51	-0.99	-0.32	-0.06	-0.06	-0.09	-0.15	-0.20	-0.26	-0.41	-0.42
B1	-1.63	-1.55	-1.44	-0.95	-0.30	-0.04	-0.05	-0.08	-0.13	-0.18	-0.24	-0.38	-0.39
B1.5	-1.55	-1.48	-1.38	-0.92	-0.28	-0.04	-0.05	-0.08	-0.12	-0.17	-0.22	-0.36	-0.36
B2	-1.48	-1.41	-1.33	-0.89	-0.27	-0.04	-0.05	-0.07	-0.11	-0.15	-0.20	-0.34	-0.32
B2.5	-1.41	-1.35	-1.27	-0.86	-0.26	-0.03	-0.04	-0.06	-0.10	-0.14	-0.18	-0.32	-0.29
B3	-1.34	-1.28	-1.20	-0.83	-0.24	-0.03	-0.04	-0.06	-0.09	-0.13	-0.16	-0.30	-0.25
B4	-1.20	-1.16	-1.08	-0.77	-0.22	-0.02	-0.03	-0.04	-0.07	-0.11	-0.13	-0.26	-0.20
B5	-1.07	-1.04	-0.96	-0.71	-0.20	-0.02	-0.02	-0.03	-0.05	-0.09	-0.11	-0.22	-0.16
B6	-0.90	-0.88	-0.82	-0.66	-0.18	-0.01	-0.01	-0.01	-0.03	-0.06	-0.07	-0.16	-0.11
B7	-0.72	-0.71	-0.68	-0.61	-0.16	-0.01	0.00	0.00	-0.01	-0.03	-0.03	-0.11	-0.06
B8	-0.55	-0.56	-0.55	-0.57	-0.14	0.00	+0.01	+0.02	+0.01	-0.01	0.00	-0.06	-0.01
B9	-0.37	-0.39	-0.40	-0.52	-0.12	0.00	+0.02	+0.03	+0.03	+0.02	+0.05	0.00	+0.04
B9.5	-0.28	-0.31	-0.33	-0.49	-0.11	+0.01	+0.02	+0.04	+0.04	+0.03	+0.07	+0.03	+0.06
A0	-0.20	-0.24	-0.27	-0.47	-0.10	+0.01	+0.03	+0.05	+0.05	+0.04	+0.09	+0.05	+0.09
A1	+0.06	-0.01	-0.08	-0.41	-0.06	+0.03	+0.05	+0.07	+0.08	+0.08	+0.15	+0.14	+0.17
A2	+0.24	+0.14	+0.05	-0.37	-0.03	+0.04	+0.06	+0.09	+0.09	+0.11	+0.20	+0.20	+0.22
A3	+0.44	+0.33	+0.21	-0.32	0.00	+0.06	+0.07	+0.10	+0.12	+0.14	+0.25	+0.26	+0.29
A4	+0.63	+0.51	+0.35	-0.22	+0.03	+0.07	+0.08	+0.12	+0.15	+0.18	+0.29	+0.32	+0.36
A5	+0.81	+0.67	+0.48	-0.12	+0.08	+0.08	+0.08	+0.14	+0.19	+0.23	+0.34	+0.38	+0.42

TABLE 6

MEAN UNREDDENED 13-COLOR PHOTOMETRY, SUPERGIANTS (Ia)

Sp	*33–63*	*33–52*	*35–52*	*37–52*	*40–52*	*45–52*	*52–58*	*52–63*	*52–72*	*52–80*	*52–86*	*52–99*	*52–110*
O9	-1.97	-1.85	-1.73	-1.12	-0.41	-0.10	-0.08	-0.12	-0.19	-0.24	-0.31	-0.48	-0.47
B0	-1.83	-1.72	-1.61	-1.06	-0.33	-0.07	-0.07	-0.10	-0.16	-0.21	-0.27	-0.42	-0.42
B0.5	-1.77	-1.67	-1.56	-1.02	-0.31	-0.06	-0.06	-0.09	-0.15	-0.20	-0.25	-0.40	-0.40
B1	-1.70	-1.61	-1.50	-0.99	-0.29	-0.04	-0.06	-0.08	-0.14	-0.19	-0.24	-0.37	-0.38
B1.5	-1.65	-1.56	-1.46	-0.97	-0.28	-0.03	-0.05	-0.08	-0.13	-0.18	-0.22	-0.35	-0.37
B2	-1.58	-1.50	-1.40	-0.94	-0.26	-0.03	-0.05	-0.07	-0.12	-0.15	-0.20	-0.32	-0.33
B2.5	-1.45	-1.39	-1.31	-0.89	-0.24	-0.02	-0.04	-0.04	-0.08	-0.11	-0.15	-0.26	-0.26
B3	-1.33	-1.29	-1.22	-0.84	-0.21	-0.01	-0.03	-0.02	-0.05	-0.07	-0.10	-0.20	-0.19
B4	-1.17	-1.16	-1.10	-0.79	-0.18	0.00	-0.01	0.00	-0.01	-0.02	-0.03	-0.12	-0.10
B5	-1.07	-1.08	-1.03	-0.75	-0.16	+0.01	0.00	+0.02	+0.02	+0.02	+0.01	-0.08	-0.05
B6	-0.99	-1.01	-0.97	-0.72	-0.15	+0.01	+0.01	+0.03	+0.04	+0.04	+0.05	-0.04	-0.02
B7	-0.92	-0.95	-0.92	-0.70	-0.14	+0.02	+0.02	+0.04	+0.05	+0.07	+0.08	-0.01	+0.02
B8	-0.86	-0.90	-0.88	-0.68	-0.13	+0.02	+0.02	+0.05	+0.07	+0.09	+0.10	+0.02	+0.03
B9	-0.68	-0.75	-0.75	-0.62	-0.11	+0.04	+0.04	+0.08	+0.10	+0.12	+0.15	+0.09	+0.11
B9.5	-0.57	-0.66	-0.67	-0.58	-0.10	+0.04	+0.05	+0.09	+0.11	+0.13	+0.18	+0.14	+0.15
A0	-0.45	-0.56	-0.58	-0.54	-0.08	+0.05	+0.05	+0.10	+0.12	+0.15	+0.20	+0.18	+0.19
A1	-0.28	-0.39	-0.43	-0.51	-0.06	+0.05	+0.06	+0.11	+0.14	+0.16	+0.23	+0.22	+0.24
A2	-0.12	-0.22	-0.29	-0.47	-0.05	+0.06	+0.07	+0.12	+0.16	+0.18	+0.26	+0.25	+0.28
A3	+0.12	0.00	-0.11	-0.42	-0.02	+0.07	+0.08	+0.13	+0.18	+0.21	+0.31	+0.30	+0.34
A4	+0.35	+0.21	+0.06	-0.35	+0.01	+0.08	+0.09	+0.14	+0.21	+0.24	+0.35	+0.35	+0.40
A5	+0.59	+0.43	+0.23	-0.27	+0.04	+0.09	+0.10	+0.16	+0.24	+0.27	+0.40	+0.41	+0.46
A6	+0.81	+0.65	+0.39	-0.16	+0.06	+0.11	+0.11	+0.17	+0.26	+0.30	+0.45	+0.46	+0.51

and the reddening lines intersect the intrinsic colors at larger angles. This method differs from (c) in that only 13C photometry, 13C intrinsic colors and 13C reddening ratios are used and not *UBV* photometry. The final spectral-color relations still had to be smoothed somewhat, and the results for Sp-$(33-63)_0$ are given in Tables 2 through 6.

The results of Tables 2 through 6 cover the spectral range O9 to A7 and luminosity classes V, IV, III, Ib, and Ia. For Sp B0.5 to A5, V or IV, we estimate the errors

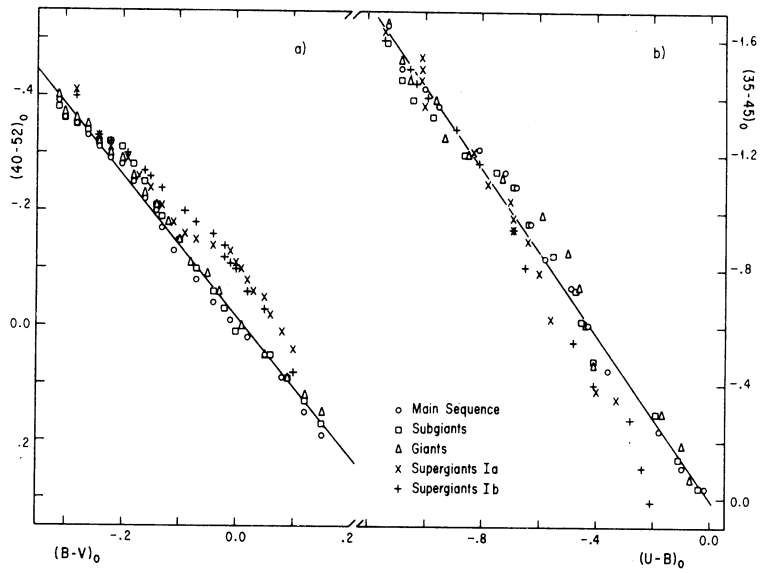

Fig. 1. Intrinsic 13C photometry versus intrinsic *UBV* photometry from Fitzgerald (1970). a) $(40-52)_0$ versus $(B-V)_0$, and b) $(35-45)_0$ versus $(U-B)_0$. Main sequence colors are shown by circles, subgiants by squares, giants by triangles, supergiants Ib by pluses, and supergiants Ia by crosses. Straight lines have been drawn to approximate the combined data of main sequence, subgiant and giant stars.

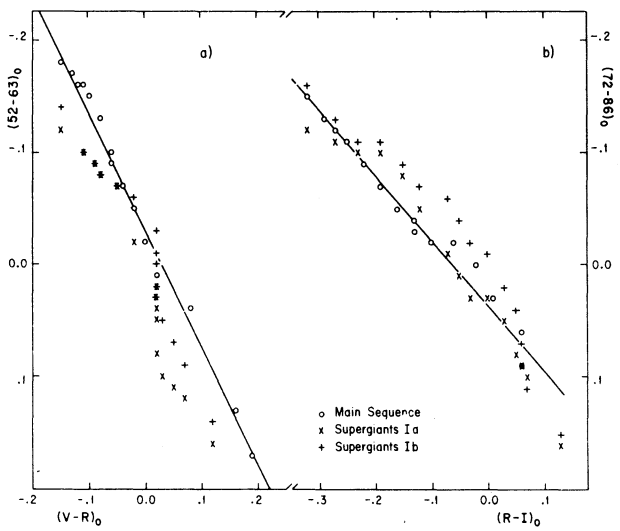

Fig. 2 Instrinsic 13C photometry versus intrinsic *VRI* photometry from Johnson (1966), a) $(52-63)_0$ versus $(V-R)_0$, and b) $(72-86)_0$ versus $(R-I)_0$. Main sequence colors are shown by circles, supergiants Ib by pluses, and supergiants Ia by crosses. Straight lines have been drawn to approximate the data of the main sequence stars.

to be ±0.02 mag (standard deviation) or less for the two-color results, and ±0.04 mag or less for the spectral-color relations. For all the giant stars and for Sp O9-B0, A6-A7, V or IV the errors are somewhat larger. Also, for Sp earlier than B6 there is a somewhat greater possibility for systematic error in the intrinsic colors due to the lack of stars within 100 parsecs. Finally, the intrinsic colors of the supergiants contain the largest errors, approximately ±0.1 mag.

In Figures 1 and 2 we plot four of our intermediate-band intrinsic colors against the intrinsic colors of *UBVRI* photometry (Fitzgerald 1970; Johnson 1966). We have selected the 13C filters to match approximately the effective wavelengths of the broad-band filters. For main sequence, subgiant, and giant colors the relationships are almost coincident and nearly linear, and we have drawn straight lines to approximate the data. The following equations give approximate transformations from 13C intrinsic colors to *UBVRI* for dwarf, subgiant, and giant stars:

$$(B-V)_0 = 0.814\,(40-52)_0 + 0.015 \quad ,$$

$$(U-B)_0 = 0.692\,(35-45)_0 - 0.003 \quad ,$$

and $$(R-I)_0 = 1.721\,(72-86)_0 - 0.064 \quad .$$

We see that for the B stars $(40-52)_0$ is more sensitive to changes in Sp, or temperature, than is $(B-V)_0$; $(45-52)_0$, not shown, is less sensitive. $(35-45)_0$ is much more sensitive than $(U-B)_0$; $(35-40)_0$ is only slightly more sensitive. $(52-63)_0$ has approximately the same range as $(V-R)_0$, and $(52-72)_0$ much more. $(72-86)_0$ has approximately half the range of $(R-I)_0$, but $(63-99)_0$ nearly 45% more. We also see in Figures 1 and 2 that the supergiants (Ia and Ib) do not follow linear relations and deviate from the less luminous stars, especially for the late-B and early-A spectral classes.

In Figure 3 are shown the relative energy distributions corresponding to the intrinsic colors from Tables 2 and 6, for main sequence and supergiant Ia stars. These have been calculated using the calibration of Johnson and

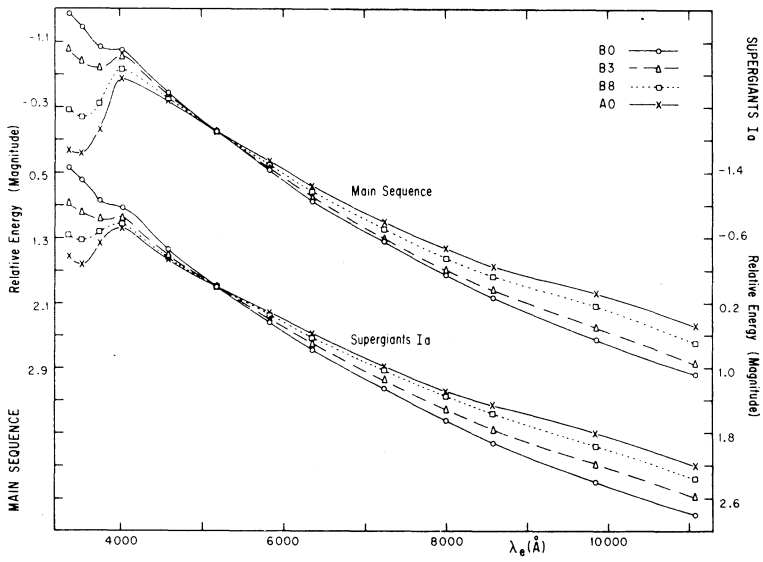

Fig. 3. Relative energies in magnitudes versus the effective wavelengths of the 13C filters for the main sequence intrinsic colors of Table 2 and for the supergiant Ia intrinsic colors of Table 6. The colors have been converted to energies using the calibration of Johnson and Mitchell (1975). Circles represent B_0 stars, triangles B3, squares B8, and crosses A_0.

Mitchell (1975) and have been plotted against the effective wavelengths of the filters. Clearly seen in filters *33*, *35*, *37* and *40* are the changes in the Balmer jump and in the Balmer lines around 3750 A due to variations in temperature and surface gravity. Also visible are smaller changes at the Paschen jump.

V. SELECTED COMPARISON STARS

Before the 13C intrinsic colors discussed above were available, individual stars were used for the computation of color excesses of Be stars (Alvarez and Schuster 1978). Normal stars with the same photospheric spectral type as the Be star were selected and dereddened, and their 13C photometry subtracted from that of the Be star to give the color excesses. Although the mean colors are now available, individual comparison stars will sometimes still be useful for differential photometric or spectroscopic studies and for model atmosphere analyses. We give in Table 7 our list of selected comparison stars, compiled using exclusively the data of Johnson and Mitchell (1975) and of Hoffleit and Jaschek (1982). We used the following criteria to select the stars: (a) non-variable, photometrically and spectroscopically; (b) normal MK spectral-luminosity classification – no evidence of emission or shell lines; (c) little interstellar reddening – $E(33-63) \leqslant +0.5$, which is equivalent to $E(B-V) \leqslant +0.2$; (d) non-contaminated 13C photometry – no fainter stars or nebulosity measured along with the comparison star; and (e) two or more observations with each photometer. Stars which do not satisfy one of the above criteria have had their bright star numbers (Hoffleit and Jaschek 1982) placed in parentheses in Table 7 and have been included in the notes.

VI. TWO-COLOR DIAGRAMS AND REDDENING-FREE INDICES

The intrinsic colors of Tables 2 through 6 serve as a basis for the study and use of classification parameters. The 13C filters span both the Balmer and Paschen jumps which are primarily temperature indicators for the B stars (Chalonge and Divan 1952). The *37* and *86* filters measure the converging Balmer and Paschen lines, respectively, which, like the Hβ index of *ubvy-β* photometry (Crawford 1978), measure the luminosities or surface gravities of B stars. By combining the filters appropriately we can obtain colors sensitive to either temperature or luminosity. If, in addition, we combine two colors using the right ratios from Table 1, we can derive indices that are both sensitive to temperature or luminosity and are also free of the effects of interstellar reddening (Johnson and Morgan 1953; Strömgren 1966).

In Figure 4 we plot, using the intrinsic colors, a two-color diagram which is rather like an H-R diagram (absolute magnitude versus spectral type). The color $(37-52)_0$ measures the luminosity-sensitive hydrogen lines near 3750 A, and $(33-63)_0$ spans the Balmer jump. This diagram *is* sensitive to interstellar reddening, but it has the interesting feature that over the spectral range B3 to B9 the reddening trajectory is parallel to the intrinsic-color loci of the main sequence, subgiant and

TABLE 7

BRIGHT STAR NUMBERS OF SELECTED COMPARISON STARS, SPECTRAL TYPES O9-A2

Sp	V	IV-V	IV	III-IV	III	II-III	II	Ib	Iab	Ia
O9	8622	...	...	...	(1899)	...	(6823)	(2782)	...	(6347)
O9.5	(1931)	...	...	...	...	...	...	(7589)	...	(1542)
	(6175)	...	...	...	...	...	...	...	...	...
B0	1855	...	...	...	1876	...	...	(6716)	...	(1903)
	6165	...	...	...	(6747)	...	...	...	...	(6822)
B0.5	1887	...	1756	...	3878	...	...	(6762)	...	(2004)
	...	...	(8797)	...	(6727)	...	...	...	...	(7482)
B1	(2648)	...	(1861)	...	(1131)	(2294)	...	(1203)	...	(130)
	5993	...	(2571)	...	(5267)	...	...	(6462)	...	
B1.5	1781	...	(5695)	...	(3468)	...	...	...	...	(7678)
	4590	...	...	...	(5469)	...	...	...	...	...
B2	(179)	(1765)	153	(1552)	(1790)	...	...	6743	...	(696)
	2344	7200	8579	...	(7591)	...	...	(8279)	...	(2135)
B2.5	(5812)	...	1810	...	...	...	...	...	...	...
	(5902)	...	7298	...	...	...	...	...	...	...
B3	(3454)	...	6588	...	8335	...	(2596)	(2240)	(2653)	(7977)
	5191	...	7426	...	...	...	...	...	...	...
B4	...	...	(1350)	...	9091	...	...	...	...	...
	...	...	7306	...	...	...	...	...	...	...
B5	3849	...	3192	...	1735	...	(3825)	(3940)	(1843)	(2827)
	8858	...	(6092)	...	7447	...	...	6714	...	...
B6	8523	...	5780	...	7358	...	...	...	...	...
	...	...	...	...	7852	...	...	...	...	...
B7	811	...	2812	...	(1791)	...	...	...	...	...
	3982	...	...	...	...	...	...	...	...	...
B8	5685	...	...	...	477	...	2657	...	...	(1713)
	8634	...	...	...	590	...	(3571)	...	...	(8020)
B9	2244	8418	7906	3970	718	...	...	...	(8143)	(1035)
	8781	8597	8976	...	8522	...	...	...	8541	...
B9.5	4757	...	...	...	(7592)	...	...	...	...	...
	9098	...	...	...	7710	...	...	...	...	...
A0	5511	...	1261	...	3981	...	(7145)	2385	...	(2074)
	6629	...	2421	...	5291	...	...	6619	...	6825
A1	875	...	3449	...	(3487)	...	...	(7835)	...	(618)
	4295	...	8641	...	...	...	...	...	...	(7573)
A2	3173	...	4033	...	5477/8	...	(2066)	(2831)	...	(7924)
	4359	...	5867	...	7371	...	...	(8345)	...	(8334)

Notes to Table 7

Symbols used

V - slightly variable, usually β CMa stars.
E - E(33-63) > +0.5.
C - photometry contaminated by fainter companion.
e - emission lines.
sh - circumstellar shell.
Sp - variable spectrum or Hα profile.
#/# - when number of 8C/6RC observations is less than 2.

BS	Notes
130	V, E, e
179	E
618	V,E,e,sh
696	E, e
1035	E, C, Sp
1131	V
1203	E
1350	V, E
1542	E, e
1552	B2III+B2IV
1713	e
1765	2/1
1790	sh
1791	sh
1843	V, E
1861	V
1899	C
1903	V, e
1931	C
2004	2/1
2066	E
2074	E
2135	E, e, Sp
2240	E
2294	V
2571	V
2596	V
2648	V
2653	Sp, 1/2
2782	V, 2/1
2827	sh, 1/1
2831	E
3454	V
3468	sh, 1/1
3487	1/1
3571	4/1
3825	1/0
3940	4/1
5267	V
5469	V, 4/1
5695	V, 4/1
5812	Sp
5902	E
6092	V
6175	V,E,e,sh
6347	E
6462	1/1
6716	E
6727	E
6747	V
6762	E
6822	E
6823	E
7145	E
7482	E, e
7573	E
7589	V
7591	1/2
7592	C
7678	V,E,e,sh
7835	E
7924	V, e
7977	V, E, e
8020	E, e, Sp
8143	V, 1/2
8279	V, E
8334	E
8345	E
8797	E

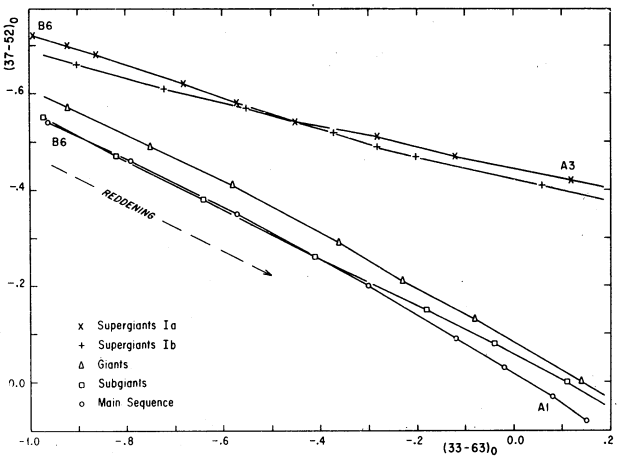

Fig. 4. The intrinsic two-color diagram, $(37-52)_0$ versus $(33-63)_0$, for late B-type and early A-type stars. The symbols have the same meaning as in Figure 1. The trajectory for interstellar reddening is show.

giant stars and is approximately parallel outside this range. We can use this two-color diagram for approximate luminosity classifications without applying reddening corrections. For Sp B1.5 to A7, we can easily distinguish main sequence, giant and supergiant stars. Figure 4 also shows that for most of the B-type stars 13C photometry *cannot* be used to separate main sequence and subgiant stars; only for Sp of approximately B9 and later do we see a significant difference in color between these two groups.

Many different combinations of the data of Table 1 with the 13C filters can be made to define reddening-free indices. For example, all of the following indices which measure the *37* filter are reddening-free, and so are possible luminosity parameters:

$$\ell = (37-45) - 0.467\,(40-58),$$

$$\lambda = (33-37) - 0.307\,(40-58),$$

and $$\beta = (37-40) - 0.355\,(40-45).$$

The following are reddening-free and temperature sensitive:

$$\tau = (35-40) - 0.304\,(40-58),$$

$$\gamma = (35-40) - 0.882\,(40-45),$$

and $$\delta = (33-35) - 0.365\,(40-45).$$

TABLE 8

THE ℓ AND τ REDDENING-FREE INDICES CALIBRATED IN TERMS OF SPECTRAL TYPES AND LUMINOSITY CLASSES

Spectral Type	Main sequence (V)		Subgiants (IV, IV-V)		Giants (III, II-III, III-IV)		Supergiants (Ib)		Supergiants (Ia)	
	ℓ	τ	ℓ	τ	ℓ	τ	ℓ	τ	ℓ	τ
O9	-.79	-1.18	-.77	-1.14	-.80	-1.20	-.78	-1.24	-.80	-1.18
B0	-.72	-1.08	-.72	-1.05	-.75	-1.10	-.75	-1.14	-.78	-1.13
B0.5	-.69	-1.03	-.69	-1.01	-.72	-1.05	-.74	-1.09	-.77	-1.10
B1	-.66	-0.98	-.66	-0.96	-.69	-1.00	-.72	-1.05	-.76	-1.08
B1.5	-.63	-0.93	-.64	-0.92	-.66	-0.95	-.71	-1.00	-.75	-1.06
B2	-.60	-0.89	-.61	-0.88	-.63	-0.90	-.69	-0.95	-.74	-1.03
B2.5	-.57	-0.84	-.58	-0.83	-.61	-0.85	-.68	-0.90	-.73	-1.01
B3	-.54	-0.79	-.55	-0.79	-.58	-0.80	-.66	-0.85	-.72	-0.99
B4	-.48	-0.69	-.50	-0.70	-.52	-0.70	-.63	-0.75	-.70	-0.94
B5	-.42	-0.60	-.44	-0.62	-.47	-0.60	-.60	-0.66	-.68	-0.88
B6	-.36	-0.50	-.38	-0.53	-.41	-0.50	-.57	-0.56	-.66	-0.82
B7	-.29	-0.40	-.33	-0.45	-.36	-0.40	-.54	-0.46	-.64	-0.76
B8	-.23	-0.31	-.26	-0.35	-.30	-0.31	-.51	-0.36	-.62	-0.70
B9	-.16	-0.16	-.17	-0.20	-.21	-0.13	-.48	-0.26	-.60	-0.62
B9.5	-.11	-0.07	-.11	-0.09	-.18	-0.06	-.47	-0.21	-.59	-0.58
A0	-.05	-0.03	-.06	0.00	-.15	0.00	-.45	-0.16	-.58	-0.52
A1	-.01	+0.02	-.01	+0.06	-.08	+0.07	-.42	-0.07	-.56	-0.38
A2	+.01	+0.02	+.01	+0.05	-.03	+0.09	-.39	+0.03	-.54	-0.25
A3	+.02	0.00	+.02	+0.01	.00	+0.08	-.36	+0.13	-.52	-0.12
A4	+.02	-0.03	+.02	-0.03	+.01	+0.06	-.33	+0.23	-.50	+0.02
A5	.00	-0.06	+.02	-0.05	+.01	+0.03	-.30	+0.33	-.48	+0.14
A6	-.01	-0.09	.00	-0.08	+.02	+0.01	-.27	+0.42	-.46	+0.28
A7	-.02	-0.12	-.04	-0.10	+.02	-0.02	-.24	+0.52	-.44	+0.41

The indices τ and γ measure the Balmer jump while δ measures the ultraviolet gradient beneath the Balmer jump. The symbols ℓ, λ and τ were chosen to suggest the physical parameters, luminosity and temperature, that they measure, while β, γ, and δ are the same indices, but with different reddening ratios, as those defined by Borgman and Blaauw (1964). We prefer ℓ over β since measurements through the *40* filter are affected by the Hδ and He absorption lines, cancelling part of β's luminosity sensitivity. In the λ parameter the *37* filter is compared to *33* on its short-wavelength side, below the Balmer jump; the observational errors will be somewhat larger. Borgman and Blaauw (1964) studied and calibrated the pair (β,δ) for MK type classification, absolute magnitudes, and intrinsic colors $[(N-M)_0 \sim (40-45)_0]$. We have studied the pairs (ℓ,τ) and (λ,γ) and will present here our results and calibrations for (ℓ,τ).

In Table 8 we give ℓ and τ calibrated in terms of MK spectral types for B- and early A-type stars, and in Figure 5 we plot the (ℓ,τ) diagram for B-type main sequence, subgiant, giant and supergiant (Ia and Ib) stars. The ℓ and τ indices have *not* been calculated from the mean colors of Tables 2-6 but have been obtained by grouping stars with equal Sp, plotting their average ℓ or τ against Sp, and then smoothing the data somewhat. We see that the (ℓ,τ) diagram is also very similar to an H-R diagram with ℓ being sensitive to changes in luminosity and τ changing most rapidly with effective temperature. This diagram is reddening-free and can be used for photometric classification to give approximate MK spectral-luminosity types.

In Tables 9 and 10 we calibrate the τ and ℓ indices in terms of effective temperature and absolute visual magnitude. The temperatures are the flux effective temperature of Underhill *et al.* (1979), who used the red part (6RC) of the 13C photometry, the energy calibration of Johnson and Mitchell (1975), fluxes predicted by model atmospheres, and the technique of Blackwell and Shallis (1977) to measure the angular diameters for O and B stars. The model atmospheres were also used to estimate the stellar fluxes at unobserved wavelengths shortward of 1380 A and longward of 11084 A. Then the integrated fluxes and angular diameters gave the flux effective temperatures according to basic definitions

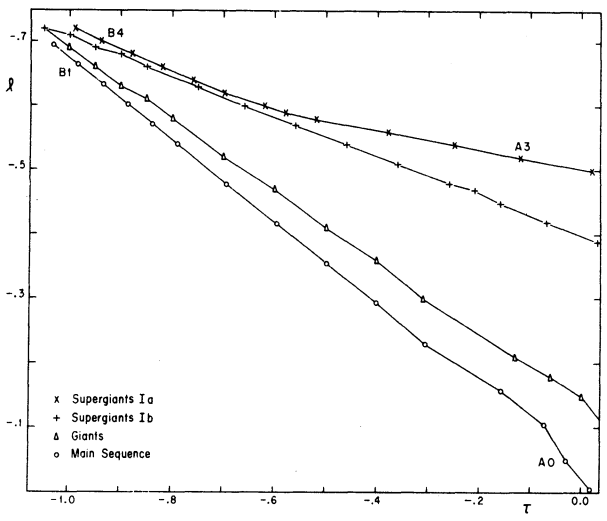

Fig. 5. The reddening-free diagram, ℓ versus τ, for the B-type stars. The indices $\ell = (37-45) - 0.467\ (40-58)$ and $\tau = (35-40) - 0.304\ (40-58)$ are independent of the average interstellar reddening according to the ratios of Table 1. The symbols have the same meaning as in Figure 1.

TABLE 9

EFFECTIVE TEMPERATURE CALIBRATION FOR τ INDEX

Main Sequence and Subgiants		Giants II, III		Supergiants Ib, I		Supergiants Ia	
τ	T_{eff}	τ	T_{eff}	τ	T_{eff}	τ	T_{eff}
-1.13	34,900	-1.12	31,900	-1.16	32,200	-1.17	32,200
-1.08	30,200	-1.06	29,100	-1.12	25,700	-1.16	28,900
-1.01	26,900	-1.01	26,800	-1.07	20,600	-1.14	23,400
-0.97	25,500	-0.96	24,500	-1.03	18,500	-1.10	20,000
-0.91	23,700	-0.90	22,100	-1.00	17,700	-1.08	18,900
-0.86	22,300	-0.86	20,700	-0.96	16,800	-1.05	17,600
-0.80	20,500	-0.80	19,200	-0.92	16,100	-0.98	15,600
-0.75	19,000	-0.70	17,100	-0.88	15,500	-0.94	14,600
-0.67	16,800	-0.60	15,400	-0.78	14,100	-0.86	13,100
-0.58	15,000	-0.50	13,800	-0.69	13,000	-0.82	12,500
-0.51	14,000	-0.40	12,300	-0.58	11,500	-0.78	12,000
-0.41	12,800	-0.30	11,400	-0.47	10,100	-0.74	11,500
-0.31	11,900	-0.17	10,800	...	...	-0.72	11,200
-0.17	10,700	-0.08	10,600	...	...	...	...
-0.06	9,900	+0.01	10,300	...	...	...	...
-0.01	9,500	...	...	...	...	...	...

TABLE 10

LUMINOSITY CALIBRATION FOR ℓ INDEX

Spectral Type	Main Sequence ℓ	Main Sequence τ	Main Sequence M_V	$\Delta M_V/\Delta\ell$[a]
B1	−0.66	−0.98	−3.6	58
B2	−0.60	−0.89	−2.5	56
B3	−0.54	−0.79	−1.7	49
B5	−0.42	−0.60	−1.0	35
B7	−0.29	−0.40	−0.4	26
B8	−0.23	−0.31	+0.1	24
B9	−0.16	−0.16	+0.6	22
A0	−0.05	−0.03	+1.0	19
A1	−0.01	+0.02	+1.5	18

a. At constant τ.

(Underhill *et al.* 1979). This temperature is defined by the total flux emitted by the star, and not by spectral line features nor by a color-index which measures only a small part of the star's spectral energy distribution. We are in fact calibrating such a color-index, which measures primarily the Balmer jump, but find a good correlation between τ and the flux effective temperature (T_{eff}).

We have plotted T_{eff} from Underhill *et al.* (1979) against τ for individual stars and give the mean relations in Table 9. The dispersion in these mean relations does not exceed ±500°K in T_{eff} for the later B stars, and ± 0.03 mag in τ for the early B stars. Such a good correlation provides strong observational evidence that the Balmer jump is in fact a good measure of the effective temperature as defined by first principles.

In Figure 5 and Table 10 we have derived a luminosity calibration for the (ℓ, τ) diagram using the absolute visual magnitudes of Blaauw (1963). For main sequence and giant stars the M_V's of Blaauw are in good agreement with those of Crawford (1978), obtained from *uvby-β* photometry of B stars in open clusters. For the main sequence calibration of Table 10 we have related the ℓ and τ values of Table 8 to the M_V of Blaauw via the Sp. The last column of Table 10 gives the average luminosity sensitivity of ℓ, the change in M_V per change in ℓ at constant τ, from class V to Ia. In general, ℓ is more sensitive to changes in M_V near the main sequence line of Figure 5 and less sensitive near the supergiant Ia line. For example, at B5 $\Delta M_V/\Delta\ell$ is 23 over the range V to III and is 39 from III to Ia.

VII. USES OF THE CALIBRATIONS

There are many uses for multifilter intermediate-band photometric systems in the study of B-type stars. Some techniques require the measurement of stellar continua over a wide wavelength range, and others depend upon the classification abilities of a few well-placed filters. For example, calibrated photometric systems can be combined with infrared and satellite ultraviolet observations to give integrated fluxes for stars, and these used to calculate bolometric corrections and effective temperatures (Johnson 1966; Underhill *et al.* 1979). Calibrated red and infrared photometries can be compared to model-atmosphere fluxes giving angular diameters and, if distances are available, linear diameters (Underhill *et al.* 1979). Relative energy curves can be used for spectral classification (Mitchell and Johnson 1969). Multiband visual systems can be combined with infrared systems for observing reddened field and cluster stars to obtain interstellar reddening curves and the ratio of total to selective absorption (Johnson 1968, 1977). The photometry of Be and shell stars can be compared to intrinsic colors to study color excesses as a function of wavelength (Johnson 1967). Reddening-free photometric indices can be used to obtain approximate MK classifications, intrinsic colors, interstellar absorptions, measures of the Balmer jump, and absolute visual magnitudes (Johnson and Morgan 1953; Becker 1963; Strömgren 1963, 1966; Borgman and Blaauw 1964; Crawford 1978). Several of the above can be combined to give photometric distances for use in galactic structure studies.

The 13C photometry and the results of this paper are applicable to all of the above. As examples, we examine in greater detail two uses –photometric distances and intrinsic color excesses–of the 13C photometry. From Figure 5 and Tables 8 and 10 we derive for a normal B-type field star a photometric MK classification and an absolute visual magnitude, M_V. From the MK type and Tables 2-6 we obtain the star's intrinsic colors. Or, more directly, once we know a star's luminosity class from Figures 4 or 5 we can calculate an intrinsic color from ℓ or τ. For example, using Tables 2 and 8,

$$(33-63)_0 = 1.603\tau - 0.149, \text{ for Sp O9 V to B7 V,}$$

and

$$(33-63)_0 = 2.064\tau + 0.036 \text{ for Sp B7 V to A1 V}$$

with very little dispersion about these two mean relations; or using Tables 6 and 8,

$$(33-63)_0 = 3.429\tau + 2.038, \text{ for Sp O9 Ia to B4 Ia,}$$

and

$$(33-63)_0 = 1.596\tau + 0.317, \text{ for Sp B4 Ia to A4 Ia}$$

with a dispersion of approximately ±0.03 mag. These relations give us $(33–63)_0$ and thus E(*33–63*) for our field star. If the star is located in a region of normal interstellar absorption, the ratio of total to selective absorption is approximately 3.1, and from Table 1, $A_V = 1.2\ E(33–63)$. We can observe the star with a *V* filter or derive an approximate *V* magnitude from $V \approx (52) - 0.5115(52–58)$ (Mitchell and Johnson 1969). From the well known relation $M_V = V + 5 - 5\ \log d - A_V$, we derive the star's distance, d, in parsecs.

To study the intrinsic excesses of Be and shell stars, we assume that the underlying star is normal and would have the intrinsic colors from Tables 2-6 corresponding to its MK classification were it not for the emission or absorption of its shell. We then select from the literature an MK spectral type for the star that was measured using criteria unaffected by the emission or shell lines, such as those of Lesh (1968). The colors from Tables 2-6 corresponding to this MK type are subtracted from the star's observed colors to give the total color excess, interstellar reddening plus intrinsic excess. We unredden the total color excess by assuming that the (*40–45*) excess is due only to interstellar reddening and apply the ratios of Table 1. This second assumption is approximately in agreement with the results of Schild (1976, 1978) and will be discussed in a later paper. In Figure 6 we plot the resulting intrinsic excesses for one shell star (BS 5941) and two Be stars (HD 53367 and BS 6118). The 13C observations for the shell star (Alvarez and Schuster 1982) are for the years 1966-68 during which the star

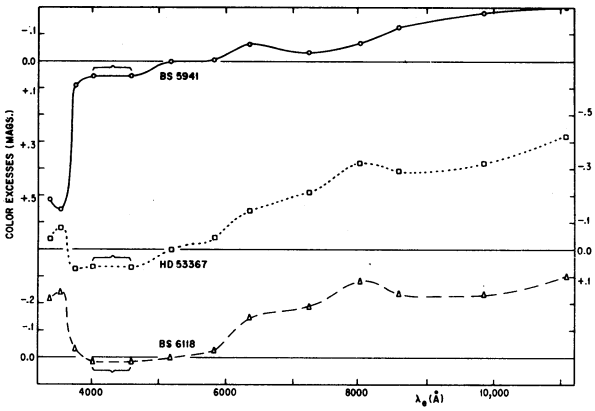

Fig. 6. Instrinsic color excesses versus the effective wavelengths of the 13C filters for one shell star (BS 5941) and two Be stars (HD 53367 and BS 6118). To correct for interstellar reddening we have assumed that the stars' (*40–45*) colors are not affected by the intrinsic excesses. Other details are given in the text.

was undergoing a shell episode. HD 53367 is a Herbig (1960) Be star, possibly pre-main sequence, and BS 6118 is a field Be star with strong emission lines ("extreme Be star"). All three stars show near-infrared excesses, and the two Be stars show an extra excess at the *80* filter which is possibly due to Paschen continuum emission or H^- processes (Schild 1978). The shell star shows a large deficiency in filters *33* and *35* due to Balmer continuum absorption in its shell, and the two Be stars have ultraviolet excesses. In the future we will apply the above techniques to many more shell and Be stars to study in detail our de-reddening assumptions, variability in the intrinsic excesses, and physical processes in the shells or emission regions.

In conclusion, we see that the 13C photometric system can be applied to many astrophysical problems. Some of the filters are well placed to measure stellar luminosities, spectral types, and interstellar reddening, and several of the blue and ultraviolet filters have been calibrated here for MK classifications, intrinsic colors, absolute visual magnitudes, and interstellar absorption. Furthermore, the 13C photometry is a multiband system giving continuum information so that effective temperatures, interstellar reddening curves, and intrinsic continuum excesses for Be stars can be obtained. In this paper we have laid the groundwork for many types of analyses of B-type stars using 13C photometry.

The author especially wishes to thank R. Mitchell for several fruitful ideas used in these analyses and R. Escamilla and A. García for help with preparation of the manuscript. I am also indebted to an anonymous referee who contributed several useful corrections. This is Contribution No. 125 of Instituto de Astronomía, UNAM.

REFERENCES

Alvarez, M. and Schuster, W. J. 1978, *Bull. AAS.*, **10**, 683.
Alvarez, M. and Schuster, W.J. 1982, *Rev. Mexicana Astron. Astrof.*, **5** 173.
Becker, W. 1963, in *Stars and Stellar Systems*, Vol. **3**, *Basic Astronomical Data*, ed. G.P. Kuiper (Chicago: The University of Chicago Press), p. 241.
Blaauw, A. 1963, in *Stars and Stellar Systems*, Vol. **3**, *Basic Astronomical Data*, ed. G.P. Kuiper (Chicago: The University of Chicago Press), p. 383.
Blackwell, D.E. and Shallis, M.J. 1977, *M.N.R.A.S.*, **180**, 177.
Borgman, J. 1960, *Bull. Astr. Inst. Netherlands*, **15**, 255.
Borgman, J. 1961, *Bull. Astr. Inst. Netherlands*, **16**, 99.
Borgman, J. and Blaauw, A. 1964, *Bull Astr. Inst. Netherlands*, **17**, 358.
Chalonge, D. and Divan, L. 1952, *Ann. d'Ap.*, **15**, 201.
Crawford, D.L. 1978, *A.J.*, **83**, 48.
Eggen, O.J. 1963, *A.J.*, **68**, 697.
Fitzgerald, M.P. 1968, *A.J.*, **73**, 983.
Fitzgerald, M.P. 1970, *Astr. and Ap.*, **4**, 234.
Herbig, G.H. 1960, *Ap. J. Suppl.*, **4**, 337.
Hoffleit, D. and Jaschek, C. 1982, *Catalogue of Bright Stars* (New Haven, Conn.: Yale University Obs.).
Jaschek, M. 1981, *Selected Spectral Types.* CDS Microfiche, Strasbourg.
Jaschek, C. and Jaschek, M. 1973, in *Spectral Classification and Multicolour Photometry, IAU Symposium 50*, eds. Ch. Fehrenbach and B.E. Westerlund (Dordrecht; D. Reidel), p. 43.
Johnson, H.L. 1966, *Ann. Rev. Astr. and Ap.*, **4**, 193.
Johnson, H.L. 1967, *Ap. J.*, **150**, L39.
Johnson, H.L. 1968, in *Stars and Stellar Systems*, Vol. **7**, *Nebulae and Interstellar Matter*, eds. B. Middlehurst and L. Aller (Chicago: The University of Chicago Press), p. 167.
Johnson, H.L. 1977, *Rev. Mexicana Astron. Astrof.*, **2**, 175.
Johnson, H.L. and Mitchell, R.I. 1975, *Rev. Mexicana Astron. Astrof.*, **1**, 299.
Johnson, H.L. and Morgan, W.W. 1953, *Ap.J.*, **117**, 313.
Johnson, H.L., Mitchell, R.I., and Latham, A.S. 1967, *Comm. Lunar and Planet. Lab.*, **6**, 85.
Johnson, H.L., Mitchell, R.I., Iriarte, B. and Wiśniewski, W.Z. 1966, *Comm. Lunar and Planet. Lab.*, **4**, 99.
Lesh, J.R. 1968, *Ap. J. Suppl.*, **17**, 371.
Mendoza, E.E. 1971, *Bol. Obs. Tonantzintla y Tacubaya*, **6**, 73.
Mitchell, R.I. and Johnson, H.L. 1969, *Comm. Lunar and Planet. Lab.*, **8**, 1.
Nicolet, B. 1978, *Astr. and Ap. Suppl.*, **34**, 1.
Schild, R.E. 1976, in *Be and Shell Stars, IAU Symposium 70*, ed. A. Slettebak (Dordrecht: D. Reidel), p. 107.
Schild, R.E. 1978, *Ap. J. Suppl.*, **37**, 77.
Schuster, W.J. 1976, *Ph. D. Dissertation*, University of Arizona, Tucson.
Schuster, W.J. 1979*a*, *Rev. Mexicana Astron. Astrof.*, **4**, 233.
Schuster, W.J. 1979*b*, *Rev. Mexicana Astron. Astrof.*, **4**, 301.
Schuster, W.J. 1982*a*, *Rev. Mexicana Astron. Astrof.*, **5**, 137.
Schuster, W.J. 1982*b*, *Rev. Mexicana Astron. Astrof.*, **5**, 149.
Schuster, W.J. 1983, unpublished.
Schuster, W.J. and Alvarez, M. 1983, *Pub. A.S.P.*, **95**, 35.
Strömgren, B. 1963, in *Stars and Stellar Systems*, Vol. **3**, *Basic Astronomical Data*, ed. G.P. Kuiper (Chicago: The University of Chicago Press), p. 123.
Strömgren, B. 1966, *Ann. Rev. Astr. and Ap.*, **4**, 433.
Underhill, A.B., Divan, L., Prévot-Burnichon, M.-L. and Doazan, V. 1979, *M.N.R.A.S.*, **189**, 601; and *Microfiche* MN 189/1.
Whiteoak, J.B. 1966, *Ap. J.*, **144**, 305.
Whitford, A.E. 1958, *A.J.*, **63**, 201.

William J. Schuster: Observatorio Astronómico Nacional, Instituto de Astronomía, UNAM, Apartado Postal 877, 22860 Ensenada, B.C., México.